Assessing the Vertical Accuracy of Worldview-3 Stereo-extracted Digital Surface Model over Olive Groves

Fran Domazetović[1][a], Ante Šiljeg[1][b], Ivan Marić[1][c] and Mladen Jurišić[2][d]

[1]University of Zadar, Department of Geography, Trg kneza Višeslava 9, 23 000 Zadar, Croatia
[2]University of Osijek, Faculty of Agriculture, Vladimira Preloga 1, 31000, Osijek, Croatia

Keywords: Worldview-3 Stereo Imagery, UAV Photogrammetry, VHR DSMs, Vertical Accuracy.

Abstract: Worldview-3 stereo-extracted DSMs represent state-of-the-art products in the domain of satellite-based digital surface modelling. Main goal of our research was to evaluate the vertical accuracy of WV-3 derived DSMs over olive groves. Creation of high-accuracy WV-3 derived DSMs would allow efficient large scale management and protection of this valuable agricultural resource.

Vertical accuracy of WV-3 derived DSM was evaluated at two test sites within Olive Gardens of Lun (Pag Island, Croatia), through the comparison with reference UAV photogrammetry derived VHR DSM. Two test sites were selected by object-based approach, established on spectral (NDVI, VARI) and height information (digital olive models (DOMs)). While first test site covers one single, individual oldest olive tree (45 m²), second test site covers larger area (2500 m²) with dense, unattended olive trees.

Although vertical accuracy of individual olive trees still significantly deviates from reference model (RMSE = 3.604 m; MAE = 3.203 m), accuracy within larger test was much better (RMSE = 1.462 m; MAE = 1.127 m). This demonstrated that WV-3 stereo imagery has great potential for application in creation of DSMs over large scale forested areas, that would be hard to cover with field geospatial techniques (e.g. LiDAR or UAV photogrammetry).

1 INTRODUCTION

In recent years very high resolution (VHR) optical satellite stereo imagery allowed extensive extraction of digital surface models (DSMs) with application in broad range of scientific fields (Aguilar et al., 2019). With the emergence of commercial satellites (e.g. IKONOS, Pleiades, GeoEye, Worldview), stereo satellite imagery has become known as cost and time effective method for creation of DSMs over large areas (Shean et al., 2016; Goldbergs et al., 2019). Although such DSMs lack the detail and resolution of models created with field geospatial methods like LiDAR or UAV photogrammetry, they require minimal field deployment (Wang et al. 2019), thus shortening the overall modelling process. If spatial extent of created DSMs is considered, satellite stereo imagery represents relatively inexpensive data collection method, where single collected stereo-pair image covers large swaths of Earth's surface (Goldbergs et al., 2019).

Development of satellites from Worldview constellation has significantly advanced the capabilities of capturing multispectral and stereo satellite imagery with sub-meter ground sampling distance (GSD) (Aguilar et al., 2013; Aguilar et al., 2014). Currently most advanced commercial satellite is Worldview-3 (WV-3), launched in August, 2014. WV-3 provides highest commercially available spatial resolution (one 0.31 m panchromatic band and eight 1.24 m multispectral bands) of collected satellite images, along with very large daily collection capacity (up to the 1 200 000 km²) (Maxar Technologies, 2019A). Stereo imagery is collected by WV-3 on the daily basis, where images of specific locations of interest are being collected from different angles, along the in-track orbit, within minimal time interval (Maxar Technologies, 2019A). Short

[a] https://orcid.org/0000-0003-3920-6703
[b] https://orcid.org/0000-0001-6332-174X
[c] https://orcid.org/0000-0002-9723-6778
[d] https://orcid.org/0000-0002-8105-6983

collection interval between two stereo images ensures that changes (e.g. atmospheric conditions, land-cover change, moving targets, etc.) at target location are minimal, thus minimalizing the potential image matching error.

As WV-3 stereo-extracted DSMs represent state-of-the-art products in the domain of satellite-based digital surface modelling, main goal of our research was to evaluate the vertical accuracy of such DSMs over olive groves. Assessment of vertical accuracy for DSM produced from WV-3 stereo-pair image (DSM_{WV3}) was based on comparison with reference VHR DSM (DSM_{UAV}) produced with the unmanned aerial vehicle (UAV) photogrammetry. UAV photogrammetry was chosen for creation of reference DSM, as practical and cost effective geospatial method that allows creation of accurate and reliable, high-quality VHR DSMs over terrains with noticeable vegetation presence (Mohan et al., 2017; Tomaštík et al., 2017; Krause et al., 2019).

Although overall quality of DSMs derived from Worldview stereo imagery was already evaluated in some previous researches, their main focus was mostly on comparison with reference LiDAR data (Shean et al., 2016; Aguilar et al., 2019; Goldbergs et al., 2019; Nemmaoui et al., 2019; Rizeei & Pradhan, 2019) and on accuracy of extraction of various man-made structures (e.g. buildings (Qin, R., 2014), plastic greenhouses (Aguilar et al., 2019; Nemmaoui et al., 2019), etc.).

In our research we have decided to concentrate on assessment of vertical accuracy of DSM over olive groves, as important specific land cover type, that covers large areas of Mediterranean and serves as one of the main agricultural sources of income and development (Orlandi et al., 2017). Detailed DSMs of olive groves are the basis for efficient management and protection of this valuable agricultural resource, as they can provide unprecedented insight into all spatio-temporal changes that are occurring within the groves (Jiménez-Brenes et al., 2017). Therefore, possibility of application of WV-3 stereo imagery for creation of high-quality DSMs would significantly improve large scale management and protection efforts.

2 STUDY AREA

Quality of Worldview-3 extracted DSM was assessed within Olive Gardens of Lun (OGL), located on Lun peninsula at most northern part of Pag Island, Croatia (Fig. 1A).
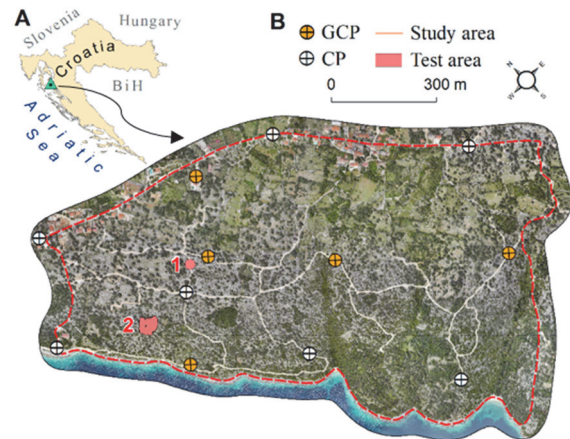

Figure 1: Location of study site within Croatia (A), location of GCPs, CPs and test sites (TA1 and TA2) within the study area (B).

OGL represents a protected olive grove that contains some of the oldest millennial olive trees in the World. As such it is protected as Sites of Community Importance (SCI), under the Natura 2000 network of European nature protection areas (European Environment Agency, 2019). Primary quality assessment (*Test site 1* (TA1)) covered one individual olive tree, that represents oldest and largest single tree within the study area. Secondary quality assessment was performed within larger test site (*Test site 2* (TA2)), covered by dense, unattended olive trees. Through primary assessment we wanted to evaluate DSM vertical accuracy for representation of individual trees, where we expected model quality to be less good. In secondary assessment we wanted to evaluate vertical accuracy of created DSM over thicker vegetation cover with larger tree crown surface, where we expected higher overall vertical accuracy. Location of test sites within the study area can be seen on Fig. 1B.

Acquisition of both WV-3 imagery and UAV aerial imagery was conducted before the seasonal pruning of the olive trees (Gucci, R. & Cantini, C., 2000), so that possible human-induced changes in height of olive trees are eliminated.

3 MATERIALS AND METHODS

3.1 Data Acquisition and Specifications

Acquisition of Worldview-3 Imagery

Worldview stereo imagery covering our study area was collected by WV-3 satellite on December 4th,

2018, within the time span of 8 minutes. Stereo images were collected at ideal conditions, with 0% cloud cover and with optimal off-NADIR angles (< 30º) (Nemmaoui et al., 2019), thus achieving claimed 5 m CE90 [1] /LE90 [2] absolute horizontal accuracy specification with 2.3 m Root Mean Square Error (RMSE) (Maxar Technologies, 2019B).

WV-3 stereo images of study area were provided to the Authors as OrthoReady Stereo imagery (OR2A), through the funding of DigitalGlobe Foundation. OR2A is radiometrically and sensor corrected imagery, that has no terrain corrections applied and is suitable for further analysis, orthorectification and elevation extraction (Maxar Technologies, 2019B). OR2A contains metadata (.STE file) required for orientation of stereo pairs in various photogrammetric software packages and creation of DSMs (Maxar Technologies, 2019B). Detailed specifications of acquired WV-3 stereo imagery are given in table 1.

Table 1: Specifications of acquired WV-3 stereo imagery.

Image ID	WV-3A	WV-3B
Image type	Stereo OR2A	Stereo OR2A
Acquisition date	04.12.2018.	04.12.2018.
Acquisition time	14:20:46	14:28:40
Off-NADIR (º)	12.1	27.1
Cloud cover (%)	0	0
GSD (m)	0.30	0.30
Scan direction	Forward	Backward
Sun azimuth (º)	157.1	157.6
Sun elevation (º)	62	62.1
Product pixel size (PAN)	0.3 m	0.3 m
Product pixel size (MS)	1.2 m	1.2 m

Aerial Survey with UAV Photogrammetry

UAV photogrammetric survey was carried out over study area on March 10th, 2019, with our newly-developed repeat aerophotogrammetric system (RAPS). RAPS represents advanced aerophotogrammetric system, composed of professional-grade DJI Matrice 600 PRO drone, Gremsy T3 gimbal, Sony Alpha A7RII (42 MP) DSLR camera equipped with 20 mm lens and Reach M+ GNSS module for UAV mapping. Due to the advanced flight capabilities and camera characteristics RAPS allows acquisition of aerial

images with very-high resolution and positioning precision.

Parameters of carried aerial surveys (double-grid flight profiles, GSD (cm), flight speed (m/s), side and forward overlap (%), etc.) were planned and automated in Universal Ground Control Software (UgCS) according to the suggestions given in Pepe et al., 2018. Flight height was set to 165 m above ground, side and forward overlap were set to 80% and GSD was 2.6 cm. Overall accuracy of DSM_{UAV} created from collected aerial images was improved with 6 fixed ground control points (GCPs) and 3 check points (CPs) distributed uniformly within the study area. GCPs and CPs were marked before the aerial survey with red paint and their precise coordinates were collected with Stonex S10 Real Time Kinematic (RTK) GPS. Survey was carried in static mode.

3.2 Data Processing and DSM Production

Creation of DSM from WV-3 Stereo Imagery

DSM of study area was created from WV-3 stereo imagery in OrthoEngine 2018 suite of Geomatica 2018 software. Workflow for DSM creation within OrthoEngine can be divided into following substeps: *math model selection* (1), *introduction of ground control points (GCPs), check points (CPs) and tie points (TPs) required for image orientation* (2), *bundle adjustment* (3), *epipolar image creation* (4) and *automatic DSM extraction* (5).

First step of DSM_{WV3} extraction includes the selection of corresponding math model (1) that serves as mathematical relationship used for correlation of two-dimensional (2D) image pixels with correct three-dimensional (3D) locations on the ground (X, Y, Z) (Barazzetti et al., 2016). Optical Satellite modeling based on provided rational polynomial coefficients (RPC) and zero-order polynomial adjustment was selected as one of the most commonly used math models for DSM extraction from WV stereo imagery (Aguilar et al., 2013; Aguilar et al., 2019; Goldbergs et al., 2019). In order to produce highly accurate DSM, introduction of GCPs (2) is required for systematic compensation of RPC induced errors and improve overall image geo-referencing accuracy (Aguilar et al., 2013; Goldbergs et al., 2019). Therefore, seven GCPs and five CPs

---

[1] CE90 - circular error at the 90th percentile, where minimum of 90 percent of the points measured has a horizontal error less than the stated CE90 value.

[2] LE90 - 90th percentile linear error, where minimum of 90 percent of vertical errors fall within the stated LE90 value.

scattered throughout the study area and surveyed with the Stonex S10 RTK-GPS were introduced, along with 187 TPs automatically detected from WV-3 stereo-pair. Reported RMSE for used GCPs, CPs and TPs is given in table 2.

Table 2: RMSE for GCPs, CPs and TPs used for creation of WV-3 stereo-derived DSM of study area.

Point type	N_0	RMSE X (m)	RMSE Y (m)	RMSE Z (m)	MEAN RMSE (m)
GCP	7	0.369	0.197	0.504	0.356
CP	5	0.320	0.517	0.737	0.525
TP	187	0.071	0.017	0.001	0.029

Introduced GCPs and TPs are then used for bundle adjustment (3) which in combination with RPC-derived sensor geometry calculates the exact position of satellite at the time of image collection. Next step covers creation of epipolar image (4), that represents stereo-pair image, where left and right images are reprojected to have common orientation and matching features distributed along the common x-axis (PCI Geomatics Enterprises, 2018).

Final step in creation of DSM_{WV3} was automated DSM extraction (5). Recent research conducted by Goldbergs et al. (2019) demonstrated that frequently used semi-global matching (SGM) is not suitable for creation of DSMs over forested areas, since it significantly underestimates tree presence and height. Therefore, in order to produce best possible quality DSM of our research area, we have tested both SGM and normalized cross-correlation (NCC) technique (both implemented within Geomatica Orthoengine 2018) for automated DSM extraction. Pixel sampling interval was set to 1 for both NCC and SGM derived DSMs, meaning that image correlation was performed at full image resolution, thus enabling extraction of fine details (e.g. bushes, trees, buildings, etc.) in created DSMs (PCI Geomatics Enterprises, 2018).

Final created DSM_{WV3} was used for orthorectification of pansharpened 8-ban multispectral WV-3 image of the study area with 0.3 m spatial resolution that was later used for extraction of vegetation cover, through OBIA approach.

Creation of DSM from UAV Photogrammetry

Aerial imagery acquired by RAPS was used for creation of VHR reference DSM of the study area in Agisoft Metashape 1.5.1. software. This software is currently one of the most advanced and precise image-based 3D modelling software that uses structure-from-motion (SfM) algorithm and multi-view 3D reconstruction technology for creation of high-quality models (Mancini et al., 2013). Workflow for extraction of VHR DSM from aerial images collected by RAPS followed the recommendations given in James et al., 2019. Based on processing of collected aerial imagery VHR reference DSM_{UAV} with 10 cm spatial resolution and digital ortophoto image (DOF) with 3 cm spatial resolution were created.

3.3 Object-based Extraction of Olive Groves

Extraction and mapping of olive groves within OGL was performed by object-based image analysis (OBIA) in eCognition Developer 9 software. OBIA extraction of olive trees was based on spectral (multispectral WV-3 image, DOF) and height information (digital olive tree models (DOMs)). DOMs were generated as difference between created DSM and corresponding digital elevation model (DEM). DEMs were created from DSM_{WV3} and DSM_{UAV} with DSM2DTM algorithm in Geomatica 2018 software.

In the first step of OBIA all olive trees within study area were extracted from the multispectral 8-band WV-3 image and created DSM_{WV3} through the use of multiresolution segmentation algorithm (MRS) (scale = 25, compactness = 0.9, shape = 0.5) and threshold-based classification (meanNDVI ≥ 0.18, meanDOMheight ≥ 0.5 m).

In second step olive trees were extracted from DOF through the same OBIA approach. While approach and MRS parameters (scale = 25, compactness = 0.9, shape = 0.5) were identical, threshold-classification had to be adjusted to different spatial and spectral resolution of UAV photogrammetry derived DSM and DOF. Since DOF is composed of only visual RGB bands, threshold classification had to be based on Visible Atmospherically Resistant Index (VARI) (meanVARI ≥ 0, meanDOMheight ≥ 0.5 m) instead of NDVI.

Two datasets of extracted olive trees were then intersected in order to derive overlapping area. Overlapping area represents the area which is covered by olive trees on both reference and WV-3 derived DSMs (Fig. 2.). As such it was taken as test area for validation of DSM_{WV3} vertical accuracy.
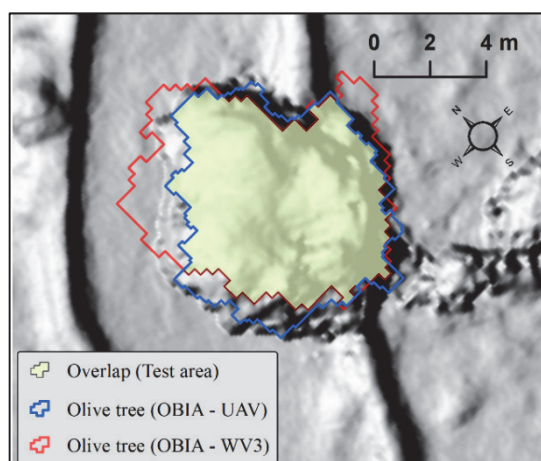
Figure 2: Test area (TA1) derived as overlap between area representing single olive tree on WV-3 and reference data.

3.4 Model Vertical Accuracy Assessment

Overall vertical accuracy of produced WV-3 DSM was assessed over olive groves with VERTICAL tool, that allows regular sampling of height values from two defined DSMs (Domazetović, 2018). VERTICAL tool samples height values along the cross-sections (Cs), in intervals that can be adjusted by the user in regard to the spatial resolution of evaluated models. For the purpose of this research both Cs and height sampling interval were set to 1 m. Sampled height values are then used for automated calculation of vertical difference (Δh) between two given DSMs, according to the following formula:

$$\Delta h = h_{WV3} - h_{UAV} \tag{1}$$

Positive values of Δh indicate that DSM_{WV3} exaggerates the height of certain point, in comparison to the reference DSM_{UAV}, while negative values are indicating underestimated height values. Neutral values ($\Delta h = 0$) indicate that at that point DSM_{WV3} does not deviates vertically from DSM_{UAV}. Vertical difference (Δh) was also used for calculation of RMSE and Mean absolute error (MAE), as representative measures of DSM_{WV3} vertical accuracy within test sites.

4 RESULTS AND DISCUSSION

4.1 Created WV-3 DSMs of Study Area

As spatial resolution of initial PAN WV-3 stereo imagery was 0.3 m and pixel sampling interval for

NCC and SGM was set to 1, spatial resolution of final created DSM_{WV3} was 0.6 m.

Although NCC and SGM approaches were based on identical input WV-3 stereo imagery and GCPs, resulting DSMs were very dissimilar. Significant differences between DSMs of study area created by NCC and SGM approaches are obvious even from basic visual comparison of created models (Fig. 3.). DSM created by SGM approach was much smoother and it lacks most of single, individual trees, thus confirming what was stated by Goldbergs et al. (2019.). On the other hand, NCC also failed to represent all individual olive trees, but representation was much better than with SGM approach.
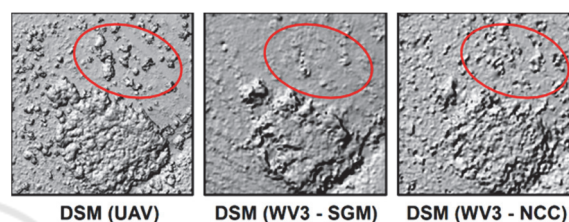

Figure 3: Visual comparison of DSMs created by NCC (*right*) and SGM (*middle*) approaches with DSM created from UAV photogrammetry (*left*); red ellipse – area covered by individual, dispersed olive trees.

While SGM was very straightforward and easy-to-use, NCC allowed higher autonomy for adjustment of user-defined parameters for DSM extraction to the local characteristics of our study area. Namely, high individual olive trees rise several meters above the surrounding terrain, significantly rising overall surface roughness. SGM technique neglected the high surface roughness and created rather smooth DSM, with very poor representation of individual olive trees. To solve this problem, we set the *smoothing filter* and *terrain type* parameters of NCC technique to *fill holes only* and *mountainous,* respectively. *Fill holes only* parameter interpolates all holes in created DSM, but does not apply any additional filtering and smoothing, which is important for preservation and representation of individual olive trees in the created model. Although terrain within our study area is represented by gentle hills, we decided to set terrain type parameter to *mountainous*, in order to preserve individual trees, that would be filtered with other two terrain type parameters (*flat, hilly*). As a result, DSM produced by NCC had much better representation of individual olive trees than DSM produced by SGM, and thus this DSM was chosen as final DSM_{WV3}.

4.2 Vertical Accuracy of WV-3 DSM

DSM_{WV3} Vertical Accuracy within TA1

Within TA1 VERTICAL tool determined the vertical difference between DSM_{WV3} and reference DSM_{UAV} in 140 height points, distributed within 8 cross-sections. It can be noted that DSM_{WV3} underestimates the height of individual olive tree crown, with negative vertical difference present in 92.857% of all sampled points. Presence of significant height underestimation is uniform within whole TA1 area. This demonstrated that although produced DSM_{WV3} managed to reproduce individual olive trees, vertical accuracy of such representation is relatively low, as it is further confirmed with RMSE and MAE values for whole TA1 (Table 3.).

DSM_{WV3} Vertical Accuracy within TA2

Within TA2 VERTICAL tool sampled 5202 height points in total, distributed within 61 cross-sections. Spatial distribution of sampled vertical transects and two exemplary vertical profiles can be seen in Fig. 4.
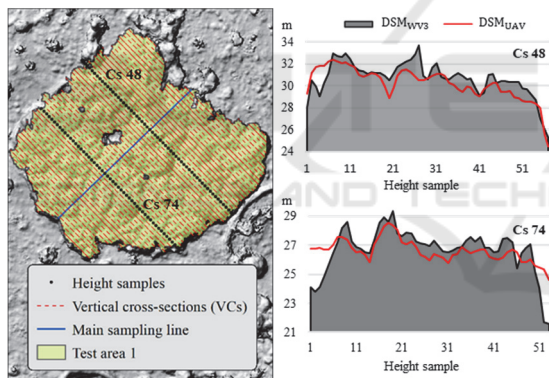

Figure 4: Spatial distribution of 61 vertical transects sampled within dense olive trees of TA2 (left); profiles of two selected vertical transects (Cs 48 & Cs 74) demonstrating visual comparison between DSM_{WV3} and reference DSM_{UAV} (right).

Unlike TA1 vertical difference between DSM_{WV3} and reference DSM_{UAV} is less pronounced within TA2. Dense, unattended crowns of olive trees within TA2 are forming relatively homogenous surface, which is much better represented within created DSM_{WV3}, than crowns of individual olive trees. Underestimation (31.311% of all sampled points) and overestimation (65.569% of all sampled points) of heights are both present in points sampled within TA2 (Fig. 5.). However, calculated RMSE and MAE values are demonstrating that overall vertical

accuracy within this test site is much higher than within TA1 (Table 3.).

Table 3: RMSE and MAE as measures of DSM_{WV3} vertical accuracy within two test areas.

Test Area	N_o of height samples	Total area (m²)	Root Mean Square Error (m)	Mean absolute error (m)
TA1	140	45	3.604	3.203
TA2	5202	2500	1.462	1.127

Better vertical accuracy within TA2 can be attributed to the characteristic of olive trees within this area, thus confirming our expectation that DSM vertical accuracy will be better for olive trees with larger and denser concentration of crowns.
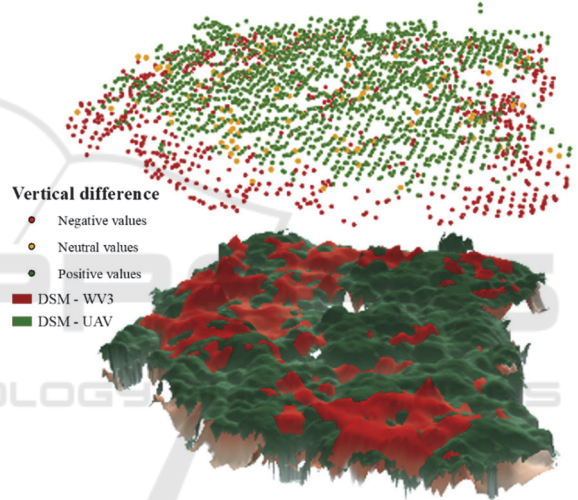

Figure 5: Vertical difference between DSM_{WV3} and DSM_{UAV} measured in 5202 height points sampled within TA2 with VERTICAL tool.

5 CONCLUSION

Main aim of our study was to evaluate the vertical accuracy and potential of WV-3 derived DSMs for application over olive groves.

Comparison of NCC and SGM approaches has demonstrated how image matching technique and user-defined parameters influence the representation of individual olive tree in produced DSMs. In overall, NCC approach with user-defined parameters adjusted to local characteristics of study area provided DSM with significantly higher representation of individual olive trees.

Although WV-3 stereo-extracted DSMs represent state-of-the-art products for satellite-based digital surface modelling, through our research we have concluded that vertical accuracy and representation of individual olive trees still significantly deviates from our reference VHR model created with UAV photogrammetry. However, if we consider that our both test sites covered very small areas and that calculated RMSE and MAE values are relatively low (in respect to spatial resolution of DSM_{WV3} and initial WV-3 stereo imagery), we can conclude that vertical accuracy of produced DSM_{WV3} is more than satisfactory.

As demonstrated by RMSE and MAE values vertical accuracy was especially good over larger test area (TA2), covered by dense, unattended olive trees. This demonstrated that WV-3 stereo imagery has great potential for application in creation of DSMs over large scale forested areas, that would be (due to high costs and terrain inaccessibility) hard to cover with field geospatial techniques (e.g. LiDAR or UAV photogrammetry).

ACKNOWLEDGEMENTS

REFERENCES

Aguilar, M. A., Bianconi, F., Aguilar, F. J., & Fernández, I. (2014). Object-based greenhouse classification from GeoEye-1 and WorldView-2 stereo imagery. *Remote sensing, 6(5), 3554-3582*.

Aguilar, M. A., del Mar Saldaña, M., & Aguilar, F. J. (2013). Generation and quality assessment of stereo-extracted DSM from GeoEye-1 and WorldView-2 imagery. *IEEE Transactions on Geoscience and Remote Sensing, 52(2), 1259-1271*.

Aguilar, M. A., Nemmaoui, A., Aguilar, F. J., & Qin, R. (2019). Quality assessment of digital surface models extracted from WorldView-2 and WorldView-3 stereo pairs over different land covers. *GIScience & remote sensing, 56(1), 109-129*.

Barazzetti, L., Roncoroni, F., Brumana, R., & Previtali, M. (2016). Georeferencing accuracy analysis of a single worldview-3 image collected over Milan. The International Archives of the Photogrammetry, *Remote Sensing and Spatial Information Sciences, Volume XLI-B1*.

Domazetović, F. (2018). Quantitative analysis of gullies of Pag island through the use of high-resolution models (Master thesis, University of Zadar. Department of Geography.).

European Environment Agency (2019.). Natura 2000 End 2018 – Shapefile. Retrived from https://www.eea.europa.eu/data-and-maps/data/natura-10/natura-2000-spatial-data/natura-2000-shapefile-1 (accessed 12 December 2019).

Goldbergs, G., Maier, S. W., Levick, S. R., & Edwards, A. (2019). Limitations of high resolution satellite stereo imagery for estimating canopy height in Australian tropical savannas. *International Journal of Applied Earth Observation and Geoinformation, 75, 83-95*.

Gucci, R., & Cantini, C. (2000). Pruning and training systems for modern olive growing. *Csiro Publishing*.

Jiménez-Brenes, F. M., López-Granados, F., de Castro, A. I., Torres-Sánchez, J., Serrano, N., & Peña, J. M. (2017). Quantifying pruning impacts on olive tree architecture and annual canopy growth by using UAV-based 3D modelling. *Plant Methods, 13(1), 55*.

Krause, S., Sanders, T. G., Mund, J. P., & Greve, K. (2019). UAV-based photogrammetric tree height measurement for intensive forest monitoring. *Remote Sensing, 11(7), 758*.

Mancini, F., Dubbini, M., Gattelli, M., Stecchi, F., Fabbri, S., & Gabbianelli, G. (2013). Using unmanned aerial vehicles (UAV) for high-resolution reconstruction of topography: The structure from motion approach on coastal environments. *Remote Sensing, 5(12), 6880-6898*.

Maxar Technologies (2019A.). Worldview-3 datasheet. Retrieved from https://www.digitalglobe.com/company/about-us (accessed 03 December 2019).

Maxar Technologies (2019A.).Stereo Imagery datasheet. Retrieved from https://www.digitalglobe.com/resources (accessed 03 December 2019).

Mohan, M., Silva, C. A., Klauberg, C., Jat, P., Catts, G., Cardil, A., ... & Dia, M. (2017). Individual tree detection from unmanned aerial vehicle (UAV) derived canopy height model in an open canopy mixed conifer forest. *Forests, 8(9), 340*.

Nemmaoui, A., Aguilar, F. J., Aguilar, M. A., & Qin, R. (2019). DSM and DTM generation from VHR satellite stereo imagery over plastic covered greenhouse areas. *Computers and Electronics in Agriculture, 164, 104903*.

Orlandi, F., Aguilera, F., Galan, C., Msallem, M., & Fornaciari, M. (2017). Olive yields forecasts and oil price trends in Mediterranean areas: a comprehensive analysis of the last two decades. *Experimental Agriculture, 53(1), 71-83*.

PCI Geomatics Enterprises (2018.). Geomatica OrthoEngine Course Exercises. Retrieved from https://www.pcigeomatics.com/pdf/TrainingGuide-Geomatica-OrthoEngine.pdf (accessed 06 Jenuary 2020).

Pepe, M., Fregonese, L., & Scaioni, M. (2018). Planning airborne photogrammetry and remote-sensing missions with modern platforms and sensors. *European Journal of Remote Sensing, 51(1), 412-436.*

Qin, R. (2014). Change detection on LOD 2 building models with very high resolution spaceborne stereo imagery. *ISPRS journal of photogrammetry and remote sensing, 96, 179-192.*

Rizeei, H. M., & Pradhan, B. (2019). Urban mapping accuracy enhancement in high-rise built-up areas deployed by 3D-orthorectification correction from WorldView-3 and LiDAR Imageries. *Remote Sensing, 11(6), 692.*

Shean, D. E., Alexandrov, O., Moratto, Z. M., Smith, B. E., Joughin, I. R., Porter, C., & Morin, P. (2016). An automated, open-source pipeline for mass production of digital elevation models (DEMs) from very-high-resolution commercial stereo satellite imagery. *ISPRS Journal of Photogrammetry and Remote Sensing, 116, 101-117.*

Tomaštík, J., Mokroš, M., Saloň, Š., Chudý, F., & Tunák, D. (2017). Accuracy of photogrammetric UAV-based point clouds under conditions of partially-open forest canopy. *Forests, 8(5), 151.*

Wang, S., Ren, Z., Wu, C., Lei, Q., Gong, W., Ou, Q., ... & Li, C. (2019). DEM generation from Worldview-2 stereo imagery and vertical accuracy assessment for its application in active tectonics. *Geomorphology, 336, 107-118.*